Highly compact, low-noise all-solid state laser system for stimulated Raman scattering microscopy

TOBIAS STEINLE[1], VIKAS KUMAR[2], ANDY STEINMANN[1], MARCO MARANGONI[2], GIULIO CERULLO[2], AND HARALD GIESSEN[1*]

[1] *4th. Physics Institute, University of Stuttgart, Germany*
[2] *IFN-CNR, Dipartimento di Fisica, Politecnico di Milano, Piazza Leonardo da Vinci 32, I-20133 Milano, Italy*
**Corresponding author: h.giessen@pi4.uni-stuttgart.de*

Received XX Month XXXX; revised XX Month, XXXX; accepted XX Month XXXX; posted XX Month XXXX (Doc. ID XXXXX); published XX Month XXXX

We present a low-noise laser system for Stimulated Raman Scattering (SRS) microscopy driven by a highly stable 8W Yb:KGW femtosecond oscillator in combination with an optical parametric amplification chain seeded by a cw laser diode. The system features easy operation, absence of any optical or electronic synchronization, wide tunability over the CH stretching region and shot-noise-limited amplitude noise at Fourier frequencies above 5 MHz. Imaging of polystyrene and PMMA micro-beads reveals its potential for SRS imaging.

OCIS codes: *(190.5650) Raman effect, (190.7110) Ultrafast nonlinear optics.*

http://dx.doi.org/10.1364/optica.99.099999

Coherent Raman Scattering (CRS) microscopy is gaining increasing recognition in biomedical optics due to its capability of non-invasive, label-free imaging of tissues and cells based on their intrinsic vibrational response [1]. CRS is a class of third-order nonlinear optical techniques making use of two synchronized trains of laser pulses at frequencies ω_P (pump frequency) and ω_S (Stokes frequency). When the difference between pump and Stokes frequencies matches a characteristic vibrational frequency Ω of a molecule, i.e. $\omega_P - \omega_S = \Omega$, all the molecules in the focal volume vibrate in phase, creating a vibrational coherence which enhances the Raman response by many orders of magnitude with respect to the incoherent, spontaneous Raman process [2]. The first CRS technique to find application was Coherent Antistokes Raman Scattering (CARS) [3, 4], which reads out the vibrational coherence by a further interaction with the pump beam, generating light at the anti-Stokes frequency $\omega_{aS} = 2\omega_P - \omega_S$. CARS has the advantage of being a background-free technique, since the anti-Stokes signal can be easily isolated by spectral filtering. On the other hand, CARS suffers from the presence of the so-called non-resonant background (NRB), generated via a four-wave-mixing process and unrelated to the targeted molecular vibration. NRB distorts and sometimes overwhelms the resonant signal of interest when the concentration of the target molecules is low. Another drawback of CARS is that, since it is a homodyne technique, its signal scales quadratically with molecular concentration.

All these limitations of CARS have been overcome by the Stimulated Raman Scattering (SRS) technique [5, 6], in which the coherent interaction with the sample induces stimulated emission from a virtual state to the investigated vibrational state, resulting in a Stokes-field amplification (Stimulated Raman Gain, SRG) and in a simultaneous pump-field attenuation (Stimulated Raman Loss, SRL). SRS is inherently free from NRB and, being a self-heterodyned technique, scales linearly with sample concentration, allowing for the detection of more dilute species and for a quantitative assessment of their concentration. Despite these important advantages in the detected signal, SRS is technologically more demanding than CARS, since it requires the measurement of a tiny differential signal (SRG or SRL) sitting on top of a large (and noisy) background given by the Stokes (or the pump) light. Extraction of this signal requires the use of sophisticated techniques, involving high-speed modulation and lock-in detection, in order to overcome the laser fluctuations.

So far, despite their unique capabilities, practical applications of CRS techniques have been confined to high-tech research laboratories. The main stumbling block preventing widespread adoption of CRS microscopy in the biological and medical communities is the complication of the experimental apparatus. CRS microscopy requires the generation of two narrowband, picosecond-duration synchronized pulse trains (pump and Stokes) with tunable frequency difference, high repetition rate (≈100 MHz) and output power >100 mW per branch, in order to overcome the losses of a typical microscope. Initial CRS implementations were based on two independent picosecond Ti:sapphire lasers, tightly synchronized by a suitable electronic active control [7], resulting in a very complex, bulky and costly set-up. A subsequent configuration, which represents the current state of the art in CRS microscopy, is based on an optical parametric oscillator (OPO) pumped by a picosecond

$Nd:YVO_4$ oscillator [8]. This system, besides its high level of complexity, still requires active cavity length synchronization between the OPO and the pump laser.

Considerable research effort is currently devoted to the development of compact fiber-format systems for CRS microscopy, with the aim of drastically reducing footprint and cost and increasing reliability. One architecture is based on a femtosecond Er:fiber oscillator, followed by two Er-doped fiber amplifiers, spectral broadening in highly nonlinear fibers and finally spectral compression via second-harmonic generation, to produce tunable pump and Stokes pulses [9-11]. This configuration has been recently upgraded by boosting the power of the Stokes arm via Yb:fiber [12] or Tm:fiber [13] amplification. An alternative scheme relies on the combination of a picosecond Yb:fiber oscillator with a fiber-based third-order optical parametric amplifier (OPA) or OPO [14-18].

Despite their clear advantages in terms of compactness and reliability, fiber lasers are difficult to be applied to SRS microscopy, because they intrinsically suffer from excess high-frequency noise with respect to their bulk counterparts [12, 18, 19]. This is due to the much greater length of the active medium, leading to more relevant contributions from amplified spontaneous emission. This prevents sensitive detection of the weak nonlinear SRS signal, sitting on top of a large linear background, and requires the adoption of balanced detection schemes [11, 12, 19] which require sophisticated noise-cancelling electronics [12] or complex optical layouts [19].

Here we present a compact, low-cost solution for SRS microscopy, based on a bulk all-solid-state Yb oscillator followed by a high repetition rate OPA. This system is simple to be operates, because the high average and peak power of the oscillator allows to directly drive nonlinear frequency conversion processes at high repetition rates. This removes the technical complications associated with the OPO or with electronic synchronization, while at the same time preserving the unsurpassed low-noise performance of bulk solid state systems. The outstanding stability of the Yb oscillator enables high quality SRS imaging without balanced detection.

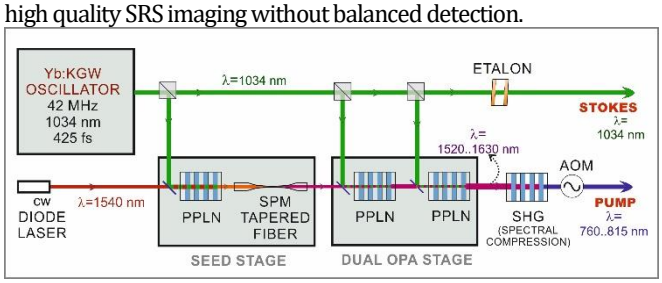

Fig. 1. Schematic diagram of the experimental system used for SRS. SPM: self-phase modulation; AOM: acousto-optic modulator. Pump beam power is >100 mW and Stokes beam power is >200 mW.

A scheme of our optical system is shown in Fig. 1. It starts with a mode-locked Yb:KGW oscillator producing 425 fs pulses at 1034 nm with 42 MHz repetition rate and 8 W average power [20]. Its RMS amplitude noise is below 0.1%, and the typical pulse-to-pulse fluctuations are around xx % over one hour. A 2-W fraction of the pulse energy is spectrally filtered by an etalon (SLS Optics Ltd.), providing a finesse of 12 and a free-spectral-range of 85 cm^{-1}, resulting in 1034 nm Stokes pulses with <10 cm^{-1} bandwidth and >200 mW average power. A 1.5 W fraction of the remaining power pumps a first OPA stage, based on a 10-mm-long MgO-doped periodically poled lithium niobate (PPLN) crystal and seeded by a cw laser diode generating 20 mW power at 1540 nm [21]. At this level of power of the seed laser, considering the repetition rate and the pulse duration of the pump laser, the seed energy per pulse is <10 fJ; this seed energy level is sufficient to completely suppress parametric superfluorescence and to overcome the energy fluctuations and timing jitter issues associated with unseeded optical parametric generation [22]. Cw seeding removes synchronization issues in the OPA and results in clean pulses with 10-nm bandwidth and 300-mW average power at 1540 nm. In the current implementation, the seed pulses are broadened by self-phase-modulation (SPM) in a tapered fiber [23] with 1.25 μm mode diameter and 8.5 cm length. The fiber output feeds two further OPA stages, based on 5 mm and 3 mm-long PPLN crystals and pumped by 1.4 and 2.5 W of the Yb:KGW, respectively, resulting in 250-fs pulses with >500 mW average power and tunability from 1520 to 1640 nm. The OPA, thanks to its seeded operation and multistage design allowing to work in saturation, displays good power stability, both short-term and long-term, with rms pulse to pulse energy fluctuations of 1.8% and average power rms fluctuations of 0.6% over one hour [21]. Finally, second-harmonic generation (SHG) spectral compression [24, also cite Fredi Leitenstorfer here] in another 20-mm-long PPLN crystal produces the <20 cm^{-1} bandwidth pump pulses, tunable from 760 to 815 nm, and allows pump-Stokes frequency detuning from 2600 to 3400 cm^{-1} with average powers in both beams of the order of 100 mW (see Fig. 2). This tuning range is fully adequate to cover the whole CH stretching region of chemical bonds, on which the vast majority of CRS applications are currently focused [1]. Note that the bandwidths of both pump and Stokes pulse can be easily adjusted to match the linewidth of the vibration of interest by selecting the etalon design and the length of the SHG crystal. Since both pump and Stokes pulses are derived from the same master Yb:KGW oscillator, they are naturally synchronized with timing jitter negligible with respect to their duration. This considerably simplifies the setup, without the need of electronic synchronization or active cavity stabilization, as in an OPO. Both pump and Stokes beam have average powers that are sufficient for SRS imaging in typical biomedical applications, taking into account the damage thresholds of cells/tissues and the typical losses of commercial microscopes.

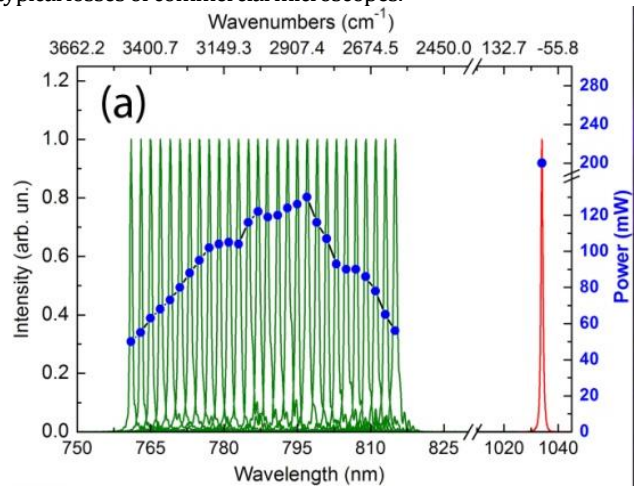

Fig. 2. Spectra of pump and Stokes pulses and corresponding average powers

Pump and Stokes beams are collinearly combined by a dichroic beam-splitter and sent to a home-made microscope (see Fig. 1(b)), employing two NA = 0.75 objectives. The pump beam is equipped with an acousto-optic amplitude modulator (Gooch&Housego) driven ata frequency of 1 MHz. The detection chain, composed of a sequence of short-pass filters, a silicon photodiode (4 MHz bandwidth) and a lock-in amplifier (SR844), filters out the modulated pump pulses and synchronously measures the SRG of the Stokes pulses. The samples are mounted on a piezo actuator

(Physik Instrumente) which limits the scan rate to 75 µm/s. We have chosen to modulate the pump beam and detect the SRG of the Stokes beam in order to exploit the exceptional stability of the bulk Yb:KGW laser. In this case, the noise floor of the measurement is mainly limited by the amplitude fluctuations of the Stokes beam; any contribution coming from the noisier pump pulse, which is generated by an OPA followed by nonlinear frequency conversion, is multiplied by the SRG transfer efficiency, which is typically 10^{-4} or less, and lies therefore well below the noise floor of the Stokes beam.

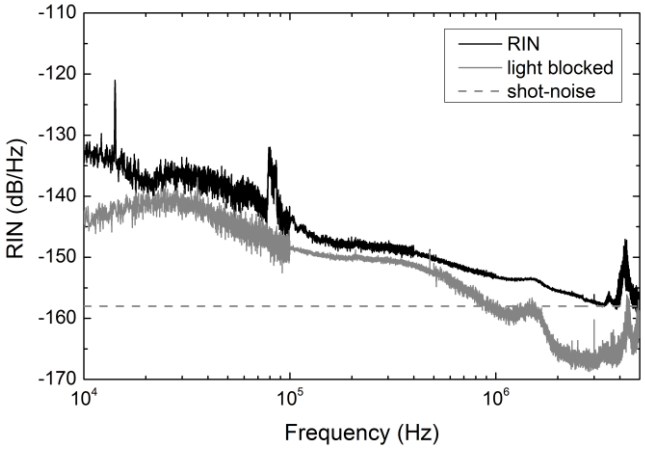

Fig. 3. RIN of the Yb:KGW pulse train. The spikes observed in the 3-4 MHz range are attributed to the electronic pre-amplifier used in the measurement. The calculated shot noise limit is -158 dB Hz^{-1} (4 mW power incident onto the detector at 1030 nm).

To estimate the sensitivity of our SRS microscope, we have measured with an electrical spectrum analyzer (Rohde&Schwarz FSL3)the relative intensity noise (RIN) spectrum of the Stokes beam, i.e. of the Yb:KGW output. The result, reported in Fig. 3, indicates that at our 1 MHz modulation frequency the RIN is -155 dB/Hz, which is within 3 dB of the shot noise limit of -158 dB/Hz. Shot-noise limited detection is achieved at modulation frequencies above 5 MHz. These values of RIN are significantly better than those achievable with current state-of-the-art fiber laser systems employed for SRS microscopy. In fact, both Freudiger *et al.* [12] and Coluccelli *et al.* [13] reported, in the 1 to 10 MHz frequency interval, RIN values that are 25÷30 dB above the shot-noise limit, while in other cases the excess noise was reported to be so high to allow only for CARS and not SRS imaging [18]. Close to shot-noise-limited performance can in principle be restored by balanced detection, in which a fraction of the signal beam is split off before the microscope and sent to the reference input of a balanced photodiode [11, 12, 19]. However, balanced detection is challenging to be implemented in a microscopy configuration, in which unavoidable transmission changes through the sample, since they are not experienced by the reference beam, produce unbalancing of the detector during the scan. This limitation can be overcome by the introduction of a more complicated yet effective auto-balanced detector design [12], which uses a variable gain amplifier to obtain an automatic match of reference and signal levels when scanning. Alternatively, a collinear balanced detection configuration can be used [19, 25], in which both probe and reference beams, after a proper delay, are collinearly transmitted through the sample. *Our system, however, achieves near shot-noise-limited performance, and allows for recording of SRS images with direct detection, avoiding all the complications of balanced detection when applied to microscopy.*

To confirm the high sensitivity of our setup, we performed SRS imaging of a blend of poly-methyl methacrylate (PMMA, 6 µm diameter) and polystyrene (PS, 3 µm diameter) beads deposited on a microscope slide. Figure 4 shows SRG images of the blend when probed at their respective Raman resonances of 2953 cm^{-1} (PMMA) and 3060 cm^{-1} (PS). Despite the relatively low value of the SRG ($<2\times10^{-5}$, due to the low damage threshold of the sample the images are extremely clean, with signal-to-noise ratio in excess of 100 without the use of balanced detection. Considering the 3 Hz noise equivalent power bandwidth of our detection chain and the measured RIN at our 1 MHz modulation frequency, we obtain an rms fluctuation of our noise floor $<10^{-7}$, in excellent agreement with the experimental noise values reported in Fig. 4.

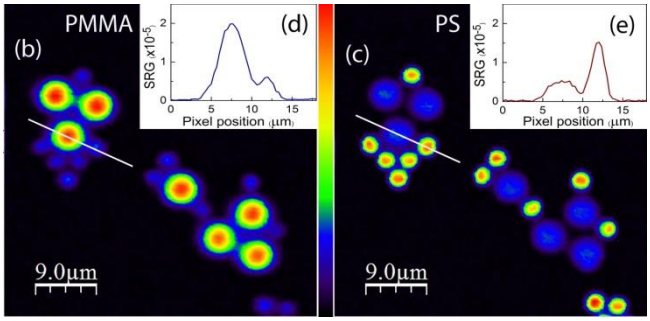

Fig. 4. (b), (c) SRS images of a blend of PMMA (6µm)and PS (3 µm) beads when probed at their respective Raman resonances of 2953 cm^{-1} (b) and 3060 cm^{-1} (c), acquired with 30-ms pixel dwell time. (d) and (e) are cross sections of the images along the solid lines.

In conclusion, we have presented a novel compact all-solid-state system for SRS microscopy, based on a bulk mode-locked Yb:KGW oscillator driving a cw-seeded OPA. The system is significantly simpler with respect to existing solutions based on bulk lasers, which require either electronic synchronization [7] or active cavity length stabilization of an OPO [8]. At the same time, the system avoids the excess high-frequency noise intrinsic in fiber lasers, allowing high-quality SRS imaging without complex balanced detection configurations. Currently, we used SPM in a tapered fiber to achieve full tunability of the OPA over the CH stretching band. In a future upgrade of the system, we plan to seed the first OPA stage by a commercially available tunable laser diode, covering the 1530-1620 nm frequency range. This will avoid SPM in the tapered fiber for tuning and simplifies the setup even further. Our system, when properly engineered, will significantly reduce the technical entrance barriers to SRS microscopy, bringing it closer to real-world biomedical applications both in research and in therapeutics.

Funding Information

We would like to thank DFG, BMBF, BW-Stiftung, Carl-Zeiss-Foundation, Alexander-von-Humboldt-Stifung, EU-COST (MP 1302), the ERC Advanced Grant COMPLEXPLAS, the EU Graphene Flagship (contract no. CNECT-ICT-604391), Fondazione Cariplo (projects "New Frontiers in Plasmonic Nanosensing" from Fondazione Cariplo - Grant No. 2011-0338. And "Surface-enhanced Coherent Antistokes Raman Scattering for label-free ultra-sensitive detection" - Grant No. 2012-0904) for funding.

References

1. J.P. Pezacki, J.A. Blake, D.C. Danielson, D.C. Kennedy, R.K. Lyn and R. Singaravelu, Nature Chem. Biol. **7**, 137 (2011).
2. C. L. Evans and X.S. Xie, Annu. Rev. Anal. Chem. **883**, 1, (2008).
3. A. Zumbusch, G.R. Holtom, X.S. Xie, Phys. Rev. Lett. **82**, 4142 (1999).
4. C. L. Evans, E. O. Potma, M. Puoris'haag, D. Cote, C. P. Lin, X. S. Xie, Proc. Natl. Acad. Sci. U.S.A. **102**, 16807 (2005).

5. Ch.W. Freudiger, W. Min, B.G. Saar, S. Lu, G.R. Holtom, C. He, J.C. Tsai, J.X. Kang, and X.S. Xie, Science **322**, 1857 (2008).
6. P. Nandakumar, A. Kovalev, A. Volkmer, New J. Phys. **11**, 033026 (2009).
7. E. O. Potma, D. J. Jones, J.-X. Cheng, X. S. Xie, J. Ye, Opt. Lett. **27**, 1163 (2002).
8. F. Ganikhanov, S. Carrasco, X. S. Xie, M. Katz, W. Seitz, D. Kopf, Opt. Lett. **31**, 1292 (2006).
9. G. Krauss, T. Hanke, A. Sell, D. Träutlein, A. Leitenstorfer, R. Selm, M. Winterhalder, and A. Zumbusch, Opt. Lett. **34**, 2847 (2009).
10. M. Marangoni, A. Gambetta, C. Manzoni, V. Kumar, R. Ramponi, and G. Cerullo, Opt. Lett. **34**, 3262 (2009).
11. A. Gambetta, V. Kumar, G. Grancini, D. Polli, R. Ramponi, G. Cerullo, M. Marangoni, Opt. Lett. **35**, 226 (2010).
12. Ch.W. Freudiger, W. Yang, G.R. Holtom, N. Peyghambarian, X. S. Xie, and K.Q. Kieu, Nature Photon. **8**, 153 (2014).
13. N. Coluccelli, V. Kumar, M. Cassinerio, G. Galzerano, M. Marangoni, and G. Cerullo, Opt. Lett. **39**, 3090 (2014).
14. M. Baumgartl, M. Chemnitz, C. Jauregui, T. Meyer, B. Dietzek, J. Popp, J. Limpert, and A. Tünnermann, Opt. Express 20, 4484 (2012).
15. Th. Gottschall, M. Baumgartl, A. Sagnier, J. Rothhardt, C. Jauregui, J. Limpert, and A. Tünnermann, Opt. Express 20, 12004 (2012).
16. M. Chemnitz, M. Baumgartl, T. Meyer, C. Jauregui, B. Dietzek, J. Popp, J. Limpert, and A. Tünnermann, Opt. Express 20, 26583 (2012).
17. S. Lefrancois, D. Fu, G.R. Holtom, L. Kong, W.J. Wadsworth, P. Schneider, R. Herda, A. Zach, X.S. Xie, and F.W. Wise, Opt. Lett. 37, 1652 (2012).
18. E. S. Lamb, S. Lefrancois, M. Ji, W.J. Wadsworth, X.S. Xie, and F.W. Wise, Opt. Lett. 38, 4154 (2013).
19. K. Nose, Y. Ozeki, T. Kishi, K. Sumimura, N. Nishizawa, K. Fukui, Y. Kanematsu, and K. Itoh, Opt. Express **20**, 13958 (2012).
20. A. Steinmann, B.Metzger, R. Hegenbarth, and H. Giessen, Conference on Lasers and Electro-Optics, OSA Technical Digest (CD) (Optical Society of America, 2011), paper CThAA5.
21. T. Steinle, S. Kedenburg, A. Steinmann, and H. Giessen, Opt. Lett., submitted (2014).
22. C. Manzoni, G. Cirmi, D. Brida, S. De Silvestri, and G. Cerullo, Phys. Rev. A **79**, 033818 (2009).
23. J. Teipel, K. Franke, D. Türke, F. Warken, D. Meiser, M. Leuschner, and H. Giessen, Appl. Phys. B **77**, 245 (2003).
24. M. Marangoni, D. Brida, M. Quintavalle, G. Cirmi, F. M. Pigozzo, C. Manzoni, F. Baronio, A. D. Capobianco, G. Cerullo, Opt. Express **15**, 8884 (2007).
25. K. Nose, T. Kishi, Y. Ozeki, Y. Kanematsu, H. Takata, K. Fukui, Y. Takai, K. Itoh, Jap. J. Appl. Phys. **53**, 052401 (2014).